Post-print of: Dzionk S., Ścibiorski B., Przybylski W. (2019) Problems of Flaking in Strengthening Shaft Burnishing. In: Gapiński B., Szostak M., Ivanov V. (eds) Advances in Manufacturing II. MANUFACTURING 2019. Lecture Notes in Mechanical Engineering. Springer, Cham. https://doi.org/10.1007/978-3-030-16943-5_10

PROBLEMS OF FLAKING IN STRENGTHENING SHAFT BURNISHING

Stefan DZIONK[1], Bogdan ŚCIBIORSKI[1] and Włodzimierz PRZYBYLSKI[1]*

[1] Faculty of Mechanical Engineering, Gdańsk University of Technology, G. Narutowicza Street,11/12 80-933 GDAŃSK, Poland

* Corresponding author. Corresponding author. Tel.: +0-058-347-1282 ; fax: +0-048-347-1450. E-mail address: stefan.dzionk@pg.edu.pl

Abstract: The article presents the results of testing the surface condition of shafts manufactured by a strengthening rolling burnishing process. The shafts with a hardness about 220HB were burnished with a roller with different force. Researches were carried out with particular attention to the structure of the outflowing material in the tool zone during burnishing process. The article presents the results of the examinations of burnished surfaces which were conducted for various structures after turning and with variable burnishing parameters. The structures of the surface after burnishing and turning are described with profilographs as well as with the photographs of the specimens surface.

Keywords: strengthening burnishing, flaking, surface layer

Burnishing is a surface treatment involving the plastic deformation of the surface processed by the pressing tools in the form of the rollers or sliding elements. In many cases, this process eliminates other finishing methods [1, 2] such as grinding, honing, superfinish, polishing and others. The burnishing process does not produce: chips, dust, sparks and etc. Cooling liquids aren't used because the process takes place at low temperatures. In addition, grinding of soft materials usually gives unsatisfactory results in the form of the surface structure and a clogging of the grinding wheel surface through the workpiece material further complicates the process. Burnishing techniques apply to various surfaces [3, 4] as well as various materials [5-10]. This process can be used to: increase the adhesion and homogeneity of galvanic coatings, reduction of stresses after heat or thermochemical treatment, increasing fatigue strength [11-12], reduces the coefficient of friction, reduce the wear [13-15] i.e. rubber seals, reducing thermal cracking of casting molds, increase surface parameters and the reflection of the surface [16-18] increase resistance to surface corrosion [19], improve durability part for aerospace [20] and other. Burnishing treatment process may be used as the smoothing processing, or smoothing and strengthening. Smoothing and strengthening treatment is applied to parts subjected

to fatigue load such as: smoothing and strengthening process is applied to parts subjected to fatigue load such as: wagon axles, turbine shafts, other shafts in which there are notches and others. Although that the research of this technology is carried out in theoretical [21-24] as well as practical aspects [25-28] do not have a precision reference to production applications. In this reason, conducting the burnishing process, it can easily lead to surface defects such as flaking of the material or drawing the wave in to the zone of the burnishing elements. This article presents the phenomena and possible limitations during burnishing process of strengthening.

2. Problems of strengthening burnishing

The process of strengthening burnishing is often applied to part which requires resistance to fatigue load. During this burnishing, high forces are applied which causes significant surface pressure of the material. Such process parameters result in significant deformations in the structure of the surface layer. Under the pressure of the tool, the material not only flows out form the pressure area but also creates displacements inside the surface layer. Figure 1 shows a schematic representation of the effect of

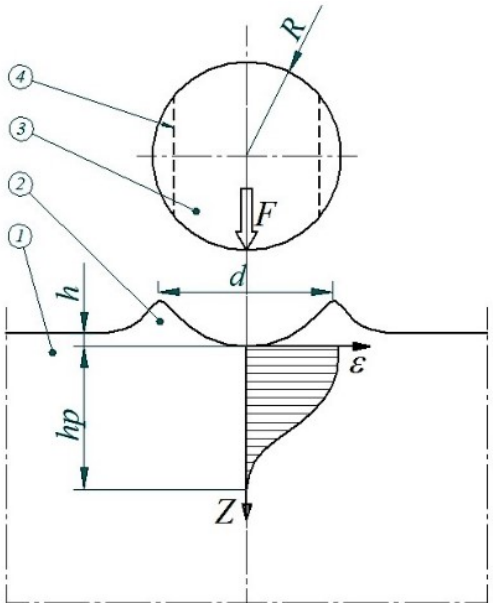

Fig. 1. Scheme of plastic deformation in the surface layer of the ball rolled shaft: 1- processing shaft, 2- flash, 3 burnishing ball, 4- line of contact boundary, ε - simple deformation, *hp* - depth of deformation, *h*- depth of trace of ball, *d*- width of ball trace, *F*- burnishing force, *R*- ball radius.

a single burnishing tool on the surface of the shaft. The penetration of the balls in the burnished material to depth (h) causes the outflow of the material around the tool in Figure 1 mark as (2) and at the same time causing the ground material to be displaced, which is illustrated by the plot of the parameter (ε).

During the movement of the burnishing tool on the surface of the shaft, the phenomena occurring during this process haven't symmetrical effects. Movement of the tool in relation to the material, which is a combination of burnishing speed and feed motion, causes that most of the flowing material accumulates in a front of the tool. Subsequent tool passes move the material along the roller and this phenomenon is called "wave" in the workshop slang. Such accumulation of material creates technological problems when its size increase put together with the length of the shaft which may result in surface defects. These surface defects mainly arise as a result of pulling in the material of wave under the burnishing elements. In this case usually there are used ways to control the size of accumulated material, e.g. by removal it using the cutting method. The flaws creating also to big material deformation degree which results flaking on the surface.

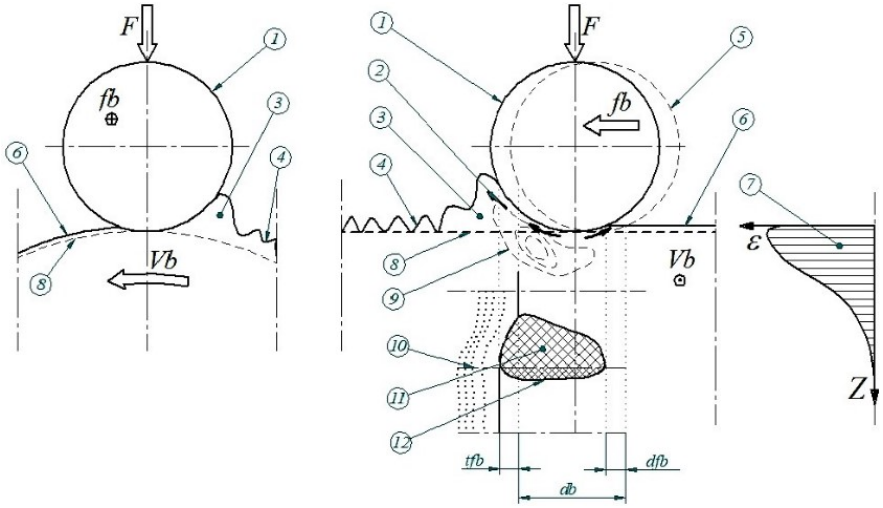

Fig. 2. Scheme of strengthening rolling burnishing: 1- burnishing ball, 2- direction of material movement during process, 3- pushing material before burnishing tool (wave), 4- surface before burnishing, 5- preceding position of ball, 6- surface after burnishing, 7- graph of deformation in the surface layer, 8- line of ball sinking, 9- zone of stresses in the surface layer, 10- surface deformation causing by pushing material (wave), 11- zone of plastic and elastic surface deformation, 12- zone of elastic deformation, *Vb*- burnishing speed, *fb*- burnishing feed rate, *F*- burnishing force, *db*- ball trace, *tfb*, *dfb* – displacement of ball trace in next pass.

Another problem is the traces left by the pressing element. The burnishing element plugging into the material causes the outflow of the burnished material. In the case of a ball movement, the outflow is unbalanced. Most of the material flows in towards the forming "wave" and the outflow in the other direction is much smaller.

In Figure 2, it shows item (*2*). This return flow of material causes that the displacement graph of the material in Figure 2 slightly differs from the graph in Figure 1. On the other hand, stop the process causes remain a trace of the burnishing element in the processed surface as a form a rounded groove cavity. The parameters of this cavity depend mainly on the shape of the processing tool and the applied burnishing force. The effects of reverse material flow are attempted to minimum by means of a special tool construction as a form of rounded cone.

3. Experimental details

The tests were performed on shafts which were processed by turning followed by burnishing. Turning and burnishing were carried out on a conventional lathe with high rigidity of the construction. The process is presented on photograph in Figure 3.

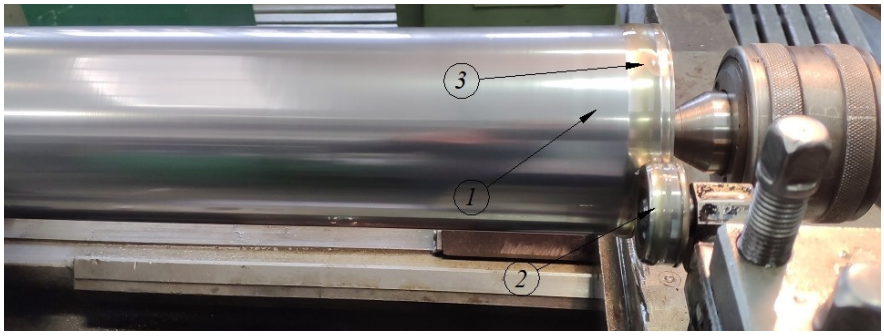

Fig. 3. Photograph of burnishing shaft: *1*- surface before burnishing, *2*- burnishing tool, *3*- surface after burnishing.

Table 1. Material data.

ISO	*EN*	*C [%]*	*Mn [%]*	*Si [%]*	*P [%]*	*Si [%]*	*Cr [%]*	*Ni [%]*	*Al [%]*	*Cu [%]*	*Hardness*
1.0562	S355	0,2	1,5	0,2-0,5	max 0,04	max 0,04	max 0,3	max 0,3	max 0,02	max 0,03	in a soft state 220HB Rm 490-630 MPa Re 335 MPa

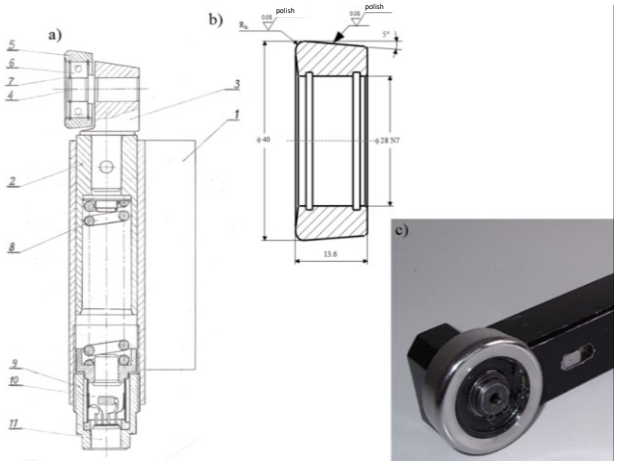

Fig. 4. Construction of burnishing tool with strain gauge way to measure burnishing force and construction of burnishing roll: a)- assembly drawing of the tool, b)- working drawing of burnishing roller, c)- photograph of the tool, 1- shank, 2- slider, 3- roller frame, 4- spindle, 5- burnishing roller, 6- ball bearing, 7-locking ring , 8- spring, 9- clamping nut, 10- strain gauge unit, 11-voltmeter connection socked.

Table 2. Processing parameters.

No of sample	*Diameter before burnishing (after turning) [mm]*	*Cutting speed Vc [m/min]*	*Feed of turning ft [mm/rev]*	*Diameter after burnishing [mm]*	*Burnishing speed Vn [m/min]*	*Feed of burnishing fn [mm/rev]*	*Force F[N]*
1	97,00	61	0,3	96,92 96,87	30,5	0,2	550
2	96,07	61	0,3	96,00	30,5	0,2	550
3	96,08	61	0,3	95,84 95,85	30,5	0,2	1150
4	96,80	61	0,3	96,70	30,5	0,2	800

Samples were made in the form of rollers with a diameter *ϕ97mm* and length *l=350mm.* The samples were made of steel 1.0562. The parameter of the processing materials presents Table 1. The samples were mounted in a three jaws self-centering chuck with the support of the rotary center. After turning, the cylindrical nature of the obtained surface was checked. Deviations on the diameter did not exceed *0.01mm* along the entire length of the shaft. The burnishing tool was mounted in a tool post. The characteristics of the burnishing tool is shown in Figure 4. The parameters of burnishing processing are presented in Table 2. In the burnishing process, machine oil type L-AN 46 (ISO 3448) was used. Profilographs were obtained

using the Hommel Tester T1000. The photographs were made by using a measuring microscope OLYMPUS SZX10.

4. Researching results and discussion

Figure 5 shows the surface profile during burnishing. The parameters of surface in both cases were the same while the burnishing force was changed. Figure 5a presents the profile of changes on the surface of the sample with a burnishing force of 500N was applied. In second case, Figure 5b shows the profile of changes on the surface for 1000N force. The shapes of both profile are similar, while the increase in force caused that both the recess (3) and the "wave" before roller (2) are about twice as large for increased force. It can also notice in the final fragment of the profile that the surface burnished with greater force has lower waviness parameters.

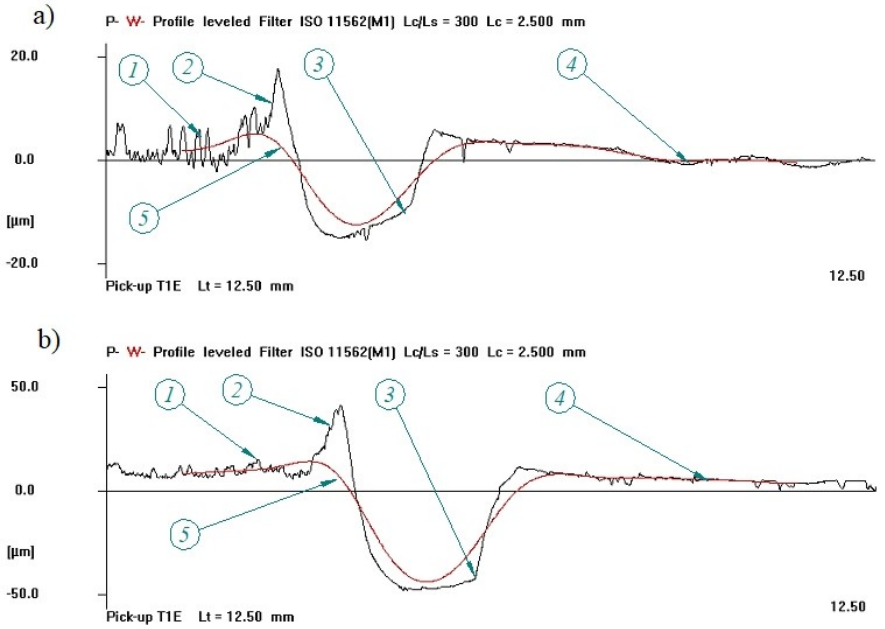

Fig. 5. Profilographs of burnishing zone: a)- for the burnishing force *F=550N*, b)- for the burnishing force *F=800N*, 1- surface before burnishing, 2- pushed material before burnishing roller, 3- squeeze of surface by the roller, 4- burnished surface.

Burnishing the shaft along the entire length caused a displacement of the material at also the front surfaces. Photograph of this material displacement is shown in Figure 6. It can be seen that the shape of the flash is similar to the graph of the dis-

placement of the material which is shown in Figure 2. This deformation was obtained with the burnishing of the cylindrical surface by the length of *350mm* and the formed wave was pushed along all length by the burnishing roller.

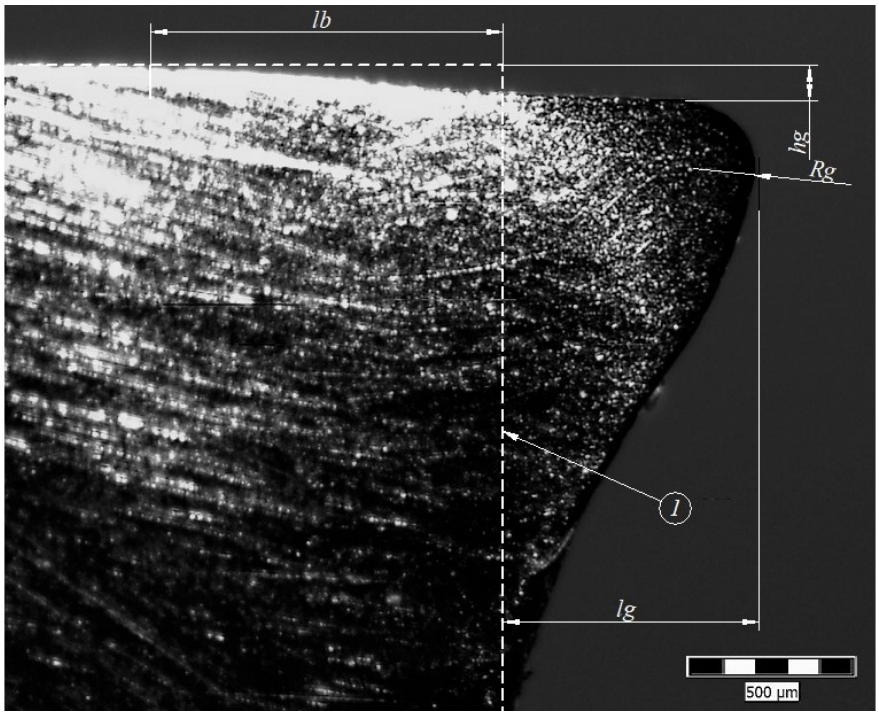

Fig. 6. Photograph of material displacement on the face surface of the shaft as the effect of burnishing peripheral surface shaft: 1- the outline of shaft before material displacement, *lg*- maximum distance of moved material, hg- concavities of the peripheral surface shaft on the displacement material, *lb*- distance of begin concaving.

In addition, the elastic pressure of the pressing element caused that in the final segment of the shaft there was a distortion deforming the diameter of the shaft. In Figure 6 at a distance of *lb* from the face of the shaft, the diameter is slightly decreases. This understating is also visible from the surface as a change the angle of reflection of light.

If too much force is applied, the material of shaft is pushed out by the burnishing roller. This material flows out under from burnishing tool and creates above the surface a ring form around the processing area. The cross-section through this phenomenon is shown in Figure 7.

Figures 8 and 9 show a photographs of the ring extruded by a roll from the tool side and from the surface before burnishing. On the side of the surface before burnishing, the surface of the ring is rough and the surfaces of the slip of the outflowed material are visible.

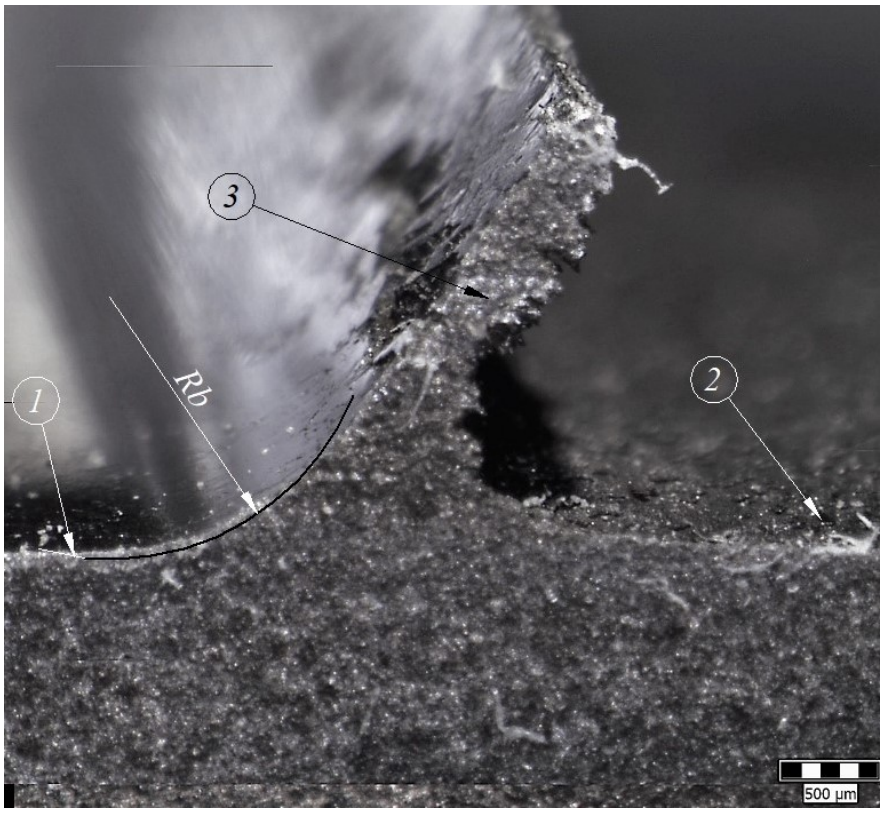

Fig. 7. Photograph of cross-section place of burnishing surface with force *F=1150N*: 1- burnished surface, 2- surface before burnishing, 3- pushing material in a front of the roller, *Rb*- radius of burnishing tool.

From the side of the burnishing tool (Figure 9), the surface of the ring is less rough and cracks are visible. Processing with such to great burnishing parameters is not recommended, if despite the fact that the burnished surface is heavily hardened and is not peeling yet. The forming ring of the material can get under the burnishing roller and lead to surface defects. In addition, the extruding material destabilizes dimensional and shape accuracy.

Figure 10 shows the surface of the shaft after strengthening burnishing. In the first phase, the process carried well (1) and the expected surface was obtained. However, in the next segment of the process, the burnishing parameters exceeded the limit values and the surface flaking took place. In this case, hard to say what caused the flaking surface and should be perform a detailed study of the properties of the workpiece relative to its homogeneity.

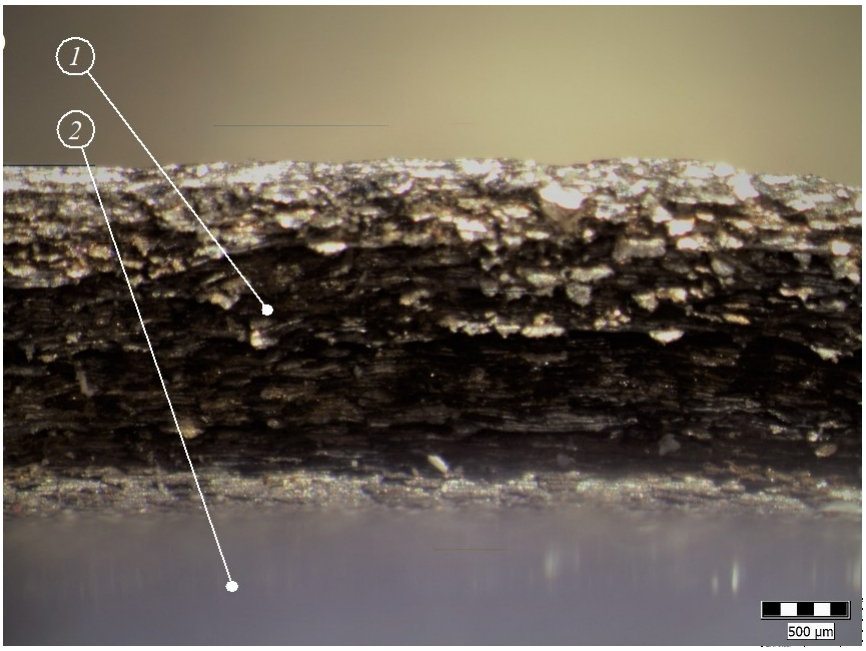

Fig. 8. Photograph of front view of pushed materials during burnishing with force *F=1150N*: front of pushed material, 2- surface before burnishing.

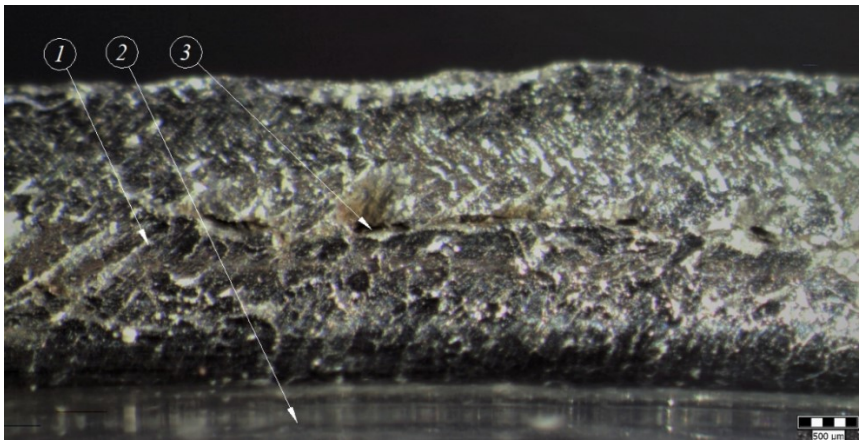

Fig. 9. Photograph of back view of pushed materials during burnishing with force F=1150N: 1- back side of pushed material, 2- surface after burnishing.

Figure 11 presents cross-section through the flaking zone. In this zone, a fragment of the peeling flake is visible which was created by a large displacement of the material in the surface layer This displacement causes the area of cracks surface (*2*) which to be seen under the flake seen in Figure 11.

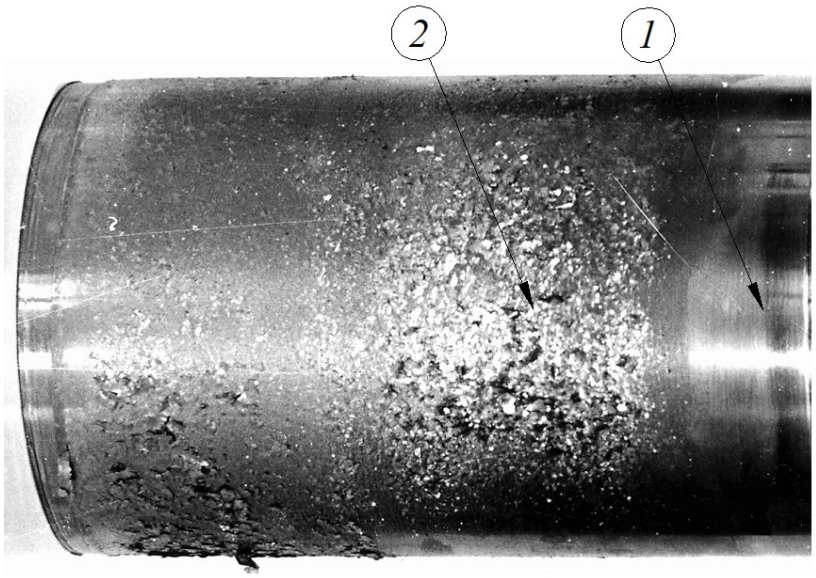

Fig. 10. Photograph of the shaft after strengthening burnishing diameter ϕ=*56mm*: 1- surface properly burnished, 2- surface with a flaking effect.

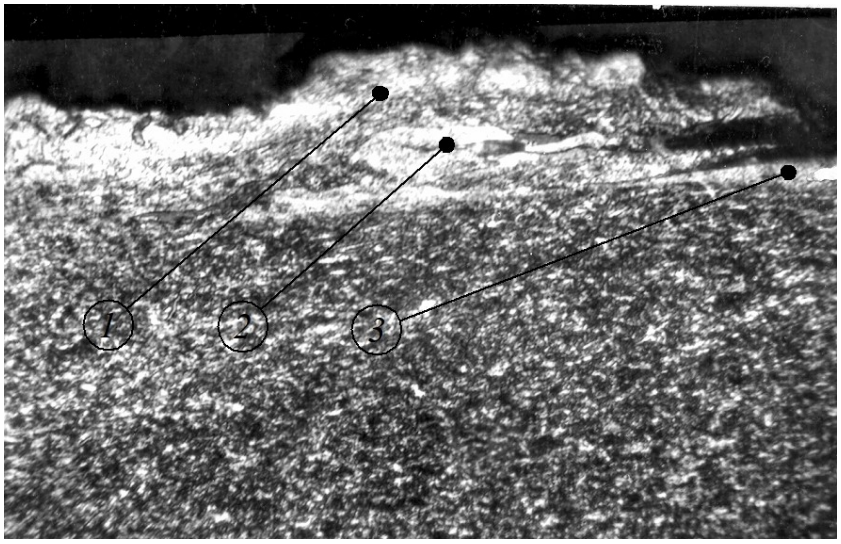

Fig. 11. Photograph of cross-section exfoliated surface: 1- creating flak on the surface, 2- micro crack, 3- actual surface after processing.

Significant displacements of the material on the surface of the burnished object are a reason the exfoliation. This process is represented also in Figure 12. This figure shows a polished and etched sample on which structure of material are visible. Large crushing and displacement of the material is visible in the grains structure of the exfoliation zone and the surface layer. The orientation of the grains elongated structure indicates that the reverse movement of material displacements occurs in the flaking zone. The material grains in this zone are much more flattened than in the deeper parts of the surface layer. In addition, they are curved shape which indicates a change in the direction of the material flow in this zone. This is marked (2) in Figure 12. It can be assumed that the strongly occurring reverse flow of the material causes significant shear stress which causes separation of the material flakes on the surface.

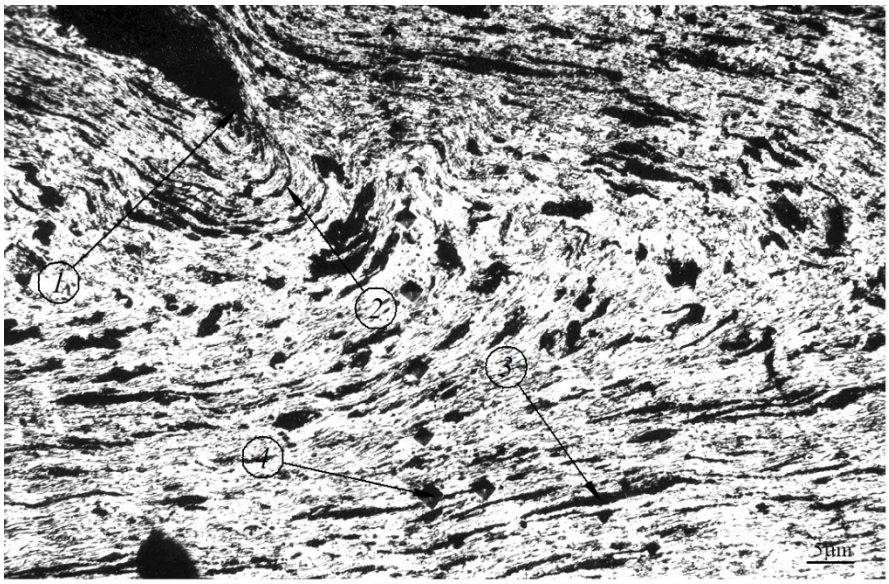

Fig. 12. Micro photograph of burnishing structure with flaking effect on the surface: 1- micro crack on the surface as a beginning of flaking , 2- the metallurgical structure of flaking zone of surface layer, 3- the metallurgical structure of grains deformation in the surface layer, 4- trace following hardness measurement.

Table 3 presents the results of micro-hardness measurements of the surface layer after burnishing. The tests were carried out for six samples at seven different depths. For this group of samples basic statistical parameters were calculated which are presented in the Table 3. The chart with the presentation of the results obtained is shown in Figure 13. It can be noticed that the changes in the surface layer of the shaft causing the increase hardness occur at depth in the range of 30-40 μm. In this range the change in the value of this parameter is about 150μHV and the its largest

decrease occurs in the depth range of 5-15µm. The highest hardness occurs in this surface zone where are large displacements of the burnished material.

Table 3. Measurement data of surface layer micro-hardness.

No of samples	*h [µm]*	*5*	*15*	*25*	*37,5*	*50*	*62,5*	*97,5*
1	µHV20i	480	350	330	320	320	320	325
2		500	350	345	320	320	320	330
		510	400	355	335	335	335	350
4		525	415	370	350	340	350	330
5		510	430	370	370	350	350	320
	$\sum_{i=1}^{n} \mu HV20i$	3035	3415	1770	2280	2035	1675	1655
	$\mu\bar{H}V_{20}$	505	427	354	347	339	336	330
	$(\mu\bar{H}V_{20} - \mu HV_{20i})^2$ µHV20-µHV2	625	5929	576	729	361	256	25
		25	5929	81	729	361	256	0
		25	729	1	144	16	1	400
		400	144	256	9	1	196	0
		25	9	256	529	121	196	
	$\sum(\mu\bar{H}V_{20} - \mu HV_{20i})^2$	1125	24847	1170	3584	1821	905	525
	$\bar{S}$	225	3560	293	718	365	227	131
	$\bar{S}^2$	15	59,6	17,1	26,8	19,1	17,1	11,5
	t_α^{n+1}	2,571	2,365	2,776	2,571	2,271	2,776	2,776
	k_α	1,050	0,896	1,238	1,050	1,050	1,238	1,238
	ε	15,75	53,5	21,2	28,1	20	53,5	21,2

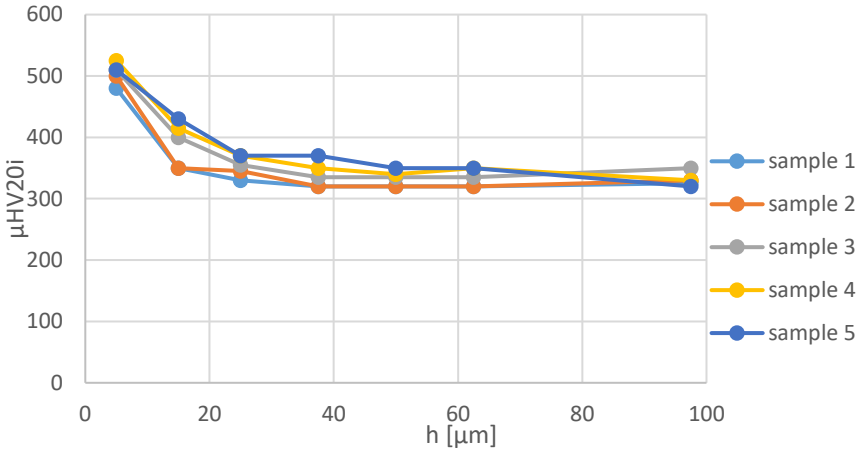

Fig. 13. Graph of micro-hardness of burnishing surface.

5. Conclusion remarks

Strengthening burnishing process enables smoothing the surface and increasing its hardness. An advantageous feature is also the compressive stresses remaining in the surface layer of the burnished component which improve its fatigue strength. However, during this process there are displacements of the material in the surface layer which results is outflows (flashes) of the material on the face surfaces of the burnished parts. The outflowing material from tool elements during the process creates a wave before the burnishing tool. Stopping the process causes that wave stays on the machined surface. In this case, there is also a roll trace remain on the surface. By increasing the burnishing force, the size of created wave at the front of the tool also increases. The increasing wave reduces the stability of the process because material creating wave may be pulled under the burnishing rollers which results in destruction of the processed part. Using a very high burnishing force, the wave takes on the shape of a thin structure separating itself from the surface which splits itself during machining. Such conducting of the machining process is incorrect because it creates a risk that the elements of the cracked material wave can get between the burnishing elements creating surface defects. In addition, with such a high pressures of burnishing elements, too much material part of the shaft is pushed out from under of the tool by decreasing its diameter after burnishing. Too much force in other burnishing conditions of the process also causes flaking of the surface. The flaking process, shape and size of wave also depend to a large extent on the type of working material and, in particular, on physical properties and metallographic structure.

References

1. Przybylski W., Dzionk S.: Hibrid processing by turning and burnishing of machine components, Advances in Manufacturing, Lecture notes in Mechanical Engineering, Springer International Publishing AG 2018, 587-598.
2. Ścibiorski B., Dzionk S.: The Roughness of the Hardened Steel Surface Created by the Rolling-Burnishing Process, Solid State Phenomena, 2015, 881-886.
3. Malarvizhi S., Chaudhari A., Woon K. S., Kumar A. S., Rahman M., Influence of Burnishing Axial Interference on Hole Surface Quality in Deep Hole Drilling of Inconel 718, Procedia Manufacturing, Volume 5, 2016, 1295-1307.
4. Korzynski M., Lubas J., Swirad S., Dudek K., Surface layer characteristics due to slide diamond burnishing with a cylindrical-ended tool, Journal of Materials Processing Technology, Volume 211, Issue 1, 2011, 84-94.
5. Okada M., Terada S., Miura T., Iwai Y., Takazawa T., Kataoka Y., Kihara T., Otsu M., Fundamental burnishing characteristics of Ni-based alloy using coated carbide tool, Procedia Manufacturing, Volume 15, 2018, 1278-1283.
6. V. Jaya Prasad, K. Sam Joshi, V.S.N. Venkata Ramana, R. Chiranjeevi, Effect of Roller Burnishing on Surface Properties of Wrought AA6063 Aluminium Alloys, Materials Today: Proceedings, Volume 5, Issue 2, Part 2, 2018, 8033-8040.
7. Grochała D., Berczyński S., Grządziel Z., Modeling of burnishing thermally toughened X42CrMo4 steel with a ceramic ZrO2 ball, Archives of Civil and Mechanical Engineering, Volume 17, Issue 4, 2017, 1011-1018.
8. Hemanth S., Harish A., R. Nithin Bharadwaj, Abhishek B Bhat, Chetan Sriharsha, Design of Roller Burnishing Tool and Its Effect on the Surface Integrity of Al 6061, Materials Today: Proceedings, Volume 5, Issue 5, Part 2, 2018, 12848-12854.
9. Pang C., Luo H., Zhang Z., Ma Y., Precipitation behavior and grain refinement of burnishing Al-Zn-Mg alloy, Progress in Natural Science: Materials International, Volume 28, Issue 1, 2018, 54-59.
10. Dzionk S., Ścibiorski B., Przybylski W.: Surface Texture Analysis of Hardened Shafts after Ceramic Ball Burnishing, Materials, Vol 12, iss 2 (2019), 1-15.
11. Fu H., Rydel J. J., R., Gola A. M., Yu F., Geng K., Lau C., Luo H., Rivera-Díaz-del-Castillo P.E.J., The relationship between 100Cr6 steelmaking, inclusion microstructure and rolling contact fatigue performance, International Journal of Fatigue, 2018, ISSN 0142-1123, https://doi.org/10.1016/j.ijfatigue.2018.11.011.
12. Manieri F., Stadler K., Morales-Espejel G.E., Kadiric A., The origins of white etching cracks and their significance to rolling bearing failures, International Journal of Fatigue, Volume 120, 2019, 107-133.
13. Pohrelyuk I.M., Sheykin S.E., Padgurskas J., Lavrys S.M., Wear resistance of two-phase titanium alloy after deformation-diffusion treatment, Tribology International, Volume 127, 2018, 404-411.
14. Johnson K.L., Contact mechanics and the wear of metals, Wear, Volume 190, Issue 2, 1995, 162-170.
15. Seo J.-W., Jun H.-K., Kwon S.-J., Lee D.-H., Rolling contact fatigue and wear of two different rail steels under rolling–sliding contact, International Journal of Fatigue, Volume 83, Part 2, 2016, 184-194.
16. Okada M., Suenobu S., Watanabe K., Yamashita Y., Asakawa N., Development and burnishing characteristics of roller burnishing method with rolling and sliding effects, Mechatronics, Volume 29, 2015, 110-118.

17. Liu Z.Y., Fu C.H., Sealy M.P., Zhao Y., Guo Y. B., Benchmark Burnishing with Almen Strip for Surface Integrity, Procedia Manufacturing, Volume 10, 2017, 456-466.
18. Li F. L., Xia W., Zhou Z. Y., Zhao J., Tang Z. Q., Analytical prediction and experimental verification of surface roughness during the burnishing process, International Journal of Machine Tools and Manufacture, Volume 62, 2012, 67-75.
19. Saldaña-Robles A., Plascencia-Mora H., Aguilera-Gómez E., Saldaña-Robles A., Marquez-Herrera A., Diosdado-De la Peña J.A., Influence of ball-burnishing on roughness, hardness and corrosion resistance of AISI 1045 steel, Surface and Coatings Technology, Volume 339, 2018, 191-198.
20. Zhang T., Bugtai N., Marinescu I. D., Burnishing of aerospace alloy: A theoretical–experimental approach, Journal of Manufacturing Systems, Volume 37, Part 2, 2015, 472-478.
21. Sebès M., Chollet H., Ayasse J.-B., Chevalier L., A multi-Hertzian contact model considering plasticity, Wear, Volume 314, Issues 1–2, 2014, 118-124.
22. Fu H., Rivera-Díaz-del-Castillo P.E.J., A unified theory for microstructural alterations in bearing steels under rolling contact fatigue, Acta Materialia, Volume 155, 2018, 43-55.
23. Fu H., Song W., Galindo-Nava E. I., Rivera-Díaz-del-Castillo P.E.J., Strain-induced martensite decay in bearing steels under rolling contact fatigue: Modelling and atomic-scale characterisation, Acta Materialia, Volume 139, 2017, 163-173.
24. Kuznetsov P., Tarasov S. Yu., Dmitriev A.I., Nanostructuring burnishing and subsurface shear instability, Journal of Materials Processing Technology, Volume 217, 2015, 327-335.
25. Jerez-Mesa R., Landon Y., Travieso-Rodriguez J.A., Dessein G., Lluma-Fuentes J., Wagner V., Topological surface integrity modification of AISI 1038 alloy after vibration-assisted ball burnishing, Surface and Coatings Technology, Volume 349, 2018, 364-377.
26. John M.R.S., Wilson A.W., Bhardwaj A.P., Abraham A., Vinayagam B.K., An investigation of ball burnishing process on CNC lathe using finite element analysis, Simulation Modelling Practice and Theory, Volume 62, 2016, 88-101.
27. Terano M., Zhang F., Yoshino M., Influence of burnishing condition on static recrystallization of an iron sheet, Procedia Engineering, Volume 207, 2017, 1850-1855.
28. Zsolt F. Kovács, Zsolt J. Viharos, János Kodácsy, Determination of the working gap and optimal machining parameters for magnetic assisted ball burnishing, Measurement, Volume 118, 2018, 172-180.